Electronic Supplementary Information (ESI) for Structural insight to halide-coordinated $[Fe_4S_4X_nY_{4-n}]^{2-}$ clusters (X, Y = Cl, Br, I) from XRD and Mössbauer spectroscopy

Andreas O. Schüren,[a,b] Benjamin M. Ridgway,[b] Florencia Di Salvo,[b,c] Luca M. Carrella,[d] Verena K. Gramm,[a] Elisa Metzger (née Rothe),[e] Fabio Doctorovich,[b,c] Eva Rentschler,[d] Volker Schünemann,[e] Uwe Ruschewitz,*[,a] Axel Klein*[,a]

[a] University zu Köln, Fakultät für Mathematik und Naturwissenschaften, Department für Chemie, Institut für Anorganische Chemie
[b] INQUIMAE-CONICET-Universidad de Buenos Aires, Intendente Güiraldes 2160, Pabellón 2, Piso 3, C1428EGA, Buenos Aires Argentina.
[c] Universidad de Buenos Aires, Facultad de Ciencias Exactas y Naturales, Departamento de Química Inorgánica, Analítica y Química Física, Intendente Güiraldes 2160, Pabellón 2, Piso 3, C1428EGA, Buenos Aires, Argentina.
[d] Johannes Gutenberg-Universität Mainz, Department Chemie, Duesbergweg 10-14, 55128 Mainz, Germany.
[e] Technische Universität Kaiserslautern, Fachbereich Physik, AG Biophysik und medizinische Physik, 67663 Kaiserslautern, Germany.

Contents:

Table S5 Selected metrics of $(BTMA)_2[Fe_4S_4X_4]$ and $(BTMA)_2[Fe_4S_4X_2Y_2]$ with X,Y = Cl, Br, I. Part I.
Table S6 Selected metrics of $(BTMA)_2[Fe_4S_4X_4]$ and $(BTMA)_2[Fe_4S_4X_2Y_2]$ with X,Y = Cl, Br, I, Part II.
Table S7 Metrical data showing the Fe_4 tetrahedron distortion and compression in $(Q)_2[Fe_4S_4X_4]$ and $(Q)_2[Fe_4S_4X_2Y_2]$ structures with X, Y = Cl, Br, I and Q = Ph_4P^+, Et_4N^+, and $n Pr_4N^+$.
Table S8 Selected crystallographic and refinement data for $(BTMA)_3[Fe_6S_6Cl_6]$ (**6**).
Table S9 Essential metrics in $[Fe_6S_6Cl_6]^{3-}$.
Table S10 Freely refined halide ratios in $(BTMA)_2[Fe_4S_4X_2Y_2]$ structures.

A - Experimental Section

Materials and procedures

The compounds were prepared and crystallised following already published procedures [1] by diffusion techniques from layered MeCN/diethyl ether mixtures at –18 °C over a period of 3 weeks. After filtration, washing with diethyl ether and drying under anaerobic and dry atmosphere (argon) using *Schlenck* techniques the opaque black rod shape crystals were stored and prepared for analytics in an argon-filled glove box at room temperature. A sample of $(BTMA)_2[Fe_4S_4I_4]$ (**5**) for Mössbauer studies was taken from the batches of the previous study.[1] The UV-vis-NIR absorption data for the compounds in MeCN solution was previously reported.[1]

$(BTMA)_2[Fe_4S_4Br_4]$ (1). Black needle-shaped crystals. **Yield:** 4.20 g (87%). **ESI-MS(–)** (acetone): m/z (%) =335.6479 (100) $[Fe_4S_4Br_4]^{2-}$, 821.4260 (60) $[BTMA+Fe_4S_4Br_4]^-$, 590.3813 (4) $[Fe_4S_4Br_3]^-$, 622.3710 (4) $[Fe_4S_4Br_3O_2]^-$, 671.2970 (4) $[Fe_4S_4Br_4]^-$, 694.2866 (2) $[Na+Fe_4S_4Br_4]^-$, 678.3131 (7) $[Li+Fe_4S_4Br_4]^-$. **Elemental analysis** for $C_{20}H_{32}Br_4Fe_4N_2S_4$ (971.37): calcd. C 24.72, H 3.32, N 2.88, S 13.20; found C 24.70, H 3.33, N 2.88, S 13.21. **FIR** (PE pellet): ν_{max} (cm^{-1}): 610 (w), 515 (w), 453 (m), 418 (w), 377 (s), 307 (s), 269 (w), 260 (sh), 227 (m), 214 (w).

$(BTMA)_2[Fe_4S_4Br_2Cl_2]$ (2) Black needle-shaped crystals. **Yield:** 7.81 g (89%). **ESI-MS(–)** (acetone): m/z (%) = 335.6492 (44) $[Fe_4S_4Br_4]^{2-}$, 313.6743 (90) $[Fe_4S_4Br_3Cl]^{2-}$, 291.6992 (100) $[Fe_4S_4Br_2Cl_2]^{2-}$, 268.7258 (19) $[Fe_4S_4BrCl_3]^{2-}$, 245.7521 (43) $[Fe_4S_4Cl_4]^{2-}$, 821.4248 (11) $[BTMA+Fe_4S_4Br_4]^-$, 777.4755 (36) $[BTMA+Fe_4S_4Br_3Cl]^-$, 731.5284 (47) $[BTMA+Fe_4S_4Br_2Cl_2]^-$, 687.5786 (27) $[BTMA+Fe_4S_4BrCl_3]^-$, 643.6280 (6) $[BTMA+Fe_4S_4Cl_4]^-$, 590.3805 (2) $[Fe_4S_4Br_3]^-$, 546.4314 (13) $[Fe_4S_4Br_2Cl]^-$, 502.4818 (24) $[Fe_4S_4BrCl_2]^-$, 456.5348 (11) $[Fe_4S_4Cl_3]^-$, 622.3699 (1) $[Fe_4S_4Br_3O_2]^-$, 578.4210 (10) $[Fe_4S_4Br_2ClO_2]^-$, 534.4714 (17) $[Fe_4S_4BrCl_2O_2]^-$, 488.5246 (8) $[Fe_4S_4Cl_3O_2]^-$. **Elemental analysis** for $C_{20}H_{32}Cl_2Br_2Fe_4N_2S_4$ (882.47): calcd. C 27.21, H 3.17, N 3.65, S 14.53; found C 27.20, H 3.18, N 3.64, S 14.55. **FIR** (PE pellet): ν_{max} (cm^{-1}): 609 (w), 515 (w), 453 (m), 419 (w), 378 (m), 356 (s), 347 (sh), 306 (s), 270 (m), 260 (sh), 233 (m).

$(BTMA)_2[Fe_4S_4Cl_2I_2]$ (3) Black needle-shaped crystals. **Yield:** 7.48 g (77%). **ESI-MS(–)** (acetone): m/z (%) = 429.6239 (42) $[Fe_4S_4I_4]^{2-}$, 383.6560 (100) $[Fe_4S_4ClI_3]^{2-}$, 337.6883 (46) $[Fe_4S_4Cl_2I_2]^{2-}$, 292.7184 (3) $[Fe_4S_4Cl_3I]^{2-}$, 245.7523 (19) $[Fe_4S_4Cl_4]^{2-}$, 1009.3728 (2) $[BTMA+Fe_4S_4I_4]^-$, 917.4389 (9) $[BTMA+Fe_4S_4ClI_3]^-$, 825.5033 (15) $[BTMA+Fe_4S_4Cl_2I_2]^-$, 733.5675 (9) $[BTMA+Fe_4S_4Cl_3I]^-$, 643.6284 (3) $[BTMA+Fe_4S_4Cl_4]^-$, 732.3404 (<1) $[Fe_4S_4I_3]^-$, 640.4057 (7) $[Fe_4S_4ClI_2]^-$, 548.4708 (21) $[Fe_4S_4Cl_2I]^-$, 456.5353 (16) $[Fe_4S_4Cl_3]^-$, 764.3302 (<1) $[Fe_4S_4I_3O_2]^-$, 672.3954 (5) $[Fe_4S_4ClI_2O_2]^-$, 580.4606 (17) $[Fe_4S_4Cl_2IO_2]^-$, 488.5251 (12) $[Fe_4S_4Cl_3O_2]^-$. **Elemental analysis** for $C_{20}H_{32}Cl_2I_2Fe_4N_2S_4$ (976.47): calcd. C 24.59, H 3.30, N 2.87, S 13.13; found C 24.57, H 3.31, N 2.88, S 13.15. **FIR** (PE pellet): ν_{max} (cm^{-1}): 609 (w), 513 (w), 452 (m), 416 (w), 378 (s), 356 (s), 346 (sh), 290 (s), 272 (m), 260 (m), 228 (m), 212 (m).

$(BTMA)_2[Fe_4S_4Br_2I_2]$ (4) Black needle-shaped crystals. **Yield:** 9.03 g (85%). **ESI-MS(–)** (acetone): m/z (%) = 429.6232 (28) $[Fe_4S_4I_4]^{2-}$, 405.6303 (72) $[Fe_4S_4BrI_3]^{2-}$, 382.6360 (96) $[Fe_4S_4Br_2I_2]^{2-}$, 359.6419 (42) $[Fe_4S_4Br_3I]^{2-}$, 335.6488 (14) $[Fe_4S_4Br_4]^{2-}$, 1009.3717 (2) $[BTMA+Fe_4S_4I_4]^-$, 961.3868 (7) $[BTMA+Fe_4S_4BrI_3]^-$, 915.3993 (14) $[BTMA+Fe_4S_4Br_2I_2]^-$, 867.4132 (9) $[BTMA+Fe_4S_4Br_3I]^-$, 821.4241 (2) $[BTMA+Fe_4S_4Br_4]^-$, 732.3395 (<1) $[Fe_4S_4I_3]^-$, 684.3543 (2) $[Fe_4S_4BrI_2]^-$, 638.3662 (5) $[Fe_4S_4Br_2I]^-$, 590.3805 (6) $[Fe_4S_4Br_3]^-$, 764.3295 (<1) $[Fe_4S_4I_3O_2]^-$, 716.3439 (1) $[Fe_4S_4BrI_2O_2]^-$, 670.3558 (4) $[Fe_4S_4Br_2IO_2]^-$, 622.3701 (4) $[Fe_4S_4Br_3O_2]^-$. **Elemental analysis** for $C_{20}H_{32}Br_2I_2Fe_4N_2S_4$ (1065.37): calcd. C 22.54, H 3.03, N 2.63, S

12.03; found C 22.55, H 3.01, N 2.61, S 12.01. **FIR** (PE pellet): ν_{max} (cm^{-1}): 609 (w), 514 (w), 452 (m), 416 (w), 376 (s), 306 (s), 291 (s), 272 (m), 260 (m), 232 (m), 210 (m).

$(BTMA)_3[Fe_6S_6Cl_6]$ (6) Black column-shaped crystals. **Yield:** 7.18 g (91%). **Elemental analysis** for $C_{30}H_{48}Cl_6Fe_6N_3S_6$ (1190.35): calcd. C 30.26, H 4.06, N 3.53, S 16.16; found C 30.30, H 4.05, N 3.51, S 16.17. **FIR** (PE pellet): ν_{max} (cm^{-1}): 612 (w), 513 (w), 454 (m), 419 (w), 381 (sh), 351 (s), 300 (m), 283 (sh), 250 (sh), 200 (w), 214 (w).

B - Supporting Figures

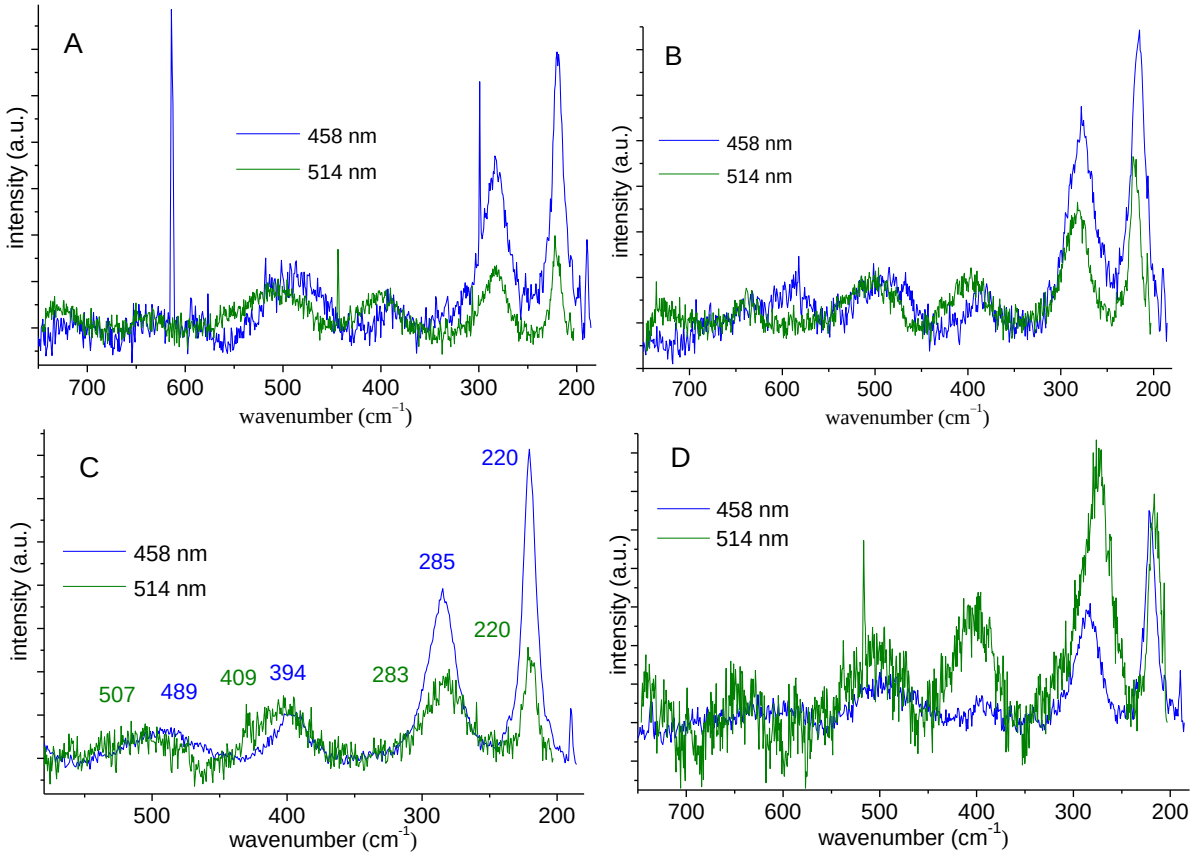

Fig. S1 Resonance Raman spectra of solid samples of $(BTMA)_2[Fe_4S_4Br_4]$ (**1**) (A), $(BTMA)_2[Fe_4S_4Br_2I_2]$ (**4**) (B), $(BTMA)_2[Fe_4S_4Br_2Cl_2]$ (**2**) (C), and $(BTMA)_2[Fe_4S_4Cl_2I_2]$ (**3**) (D) at 458 or 514 nm irradiation.

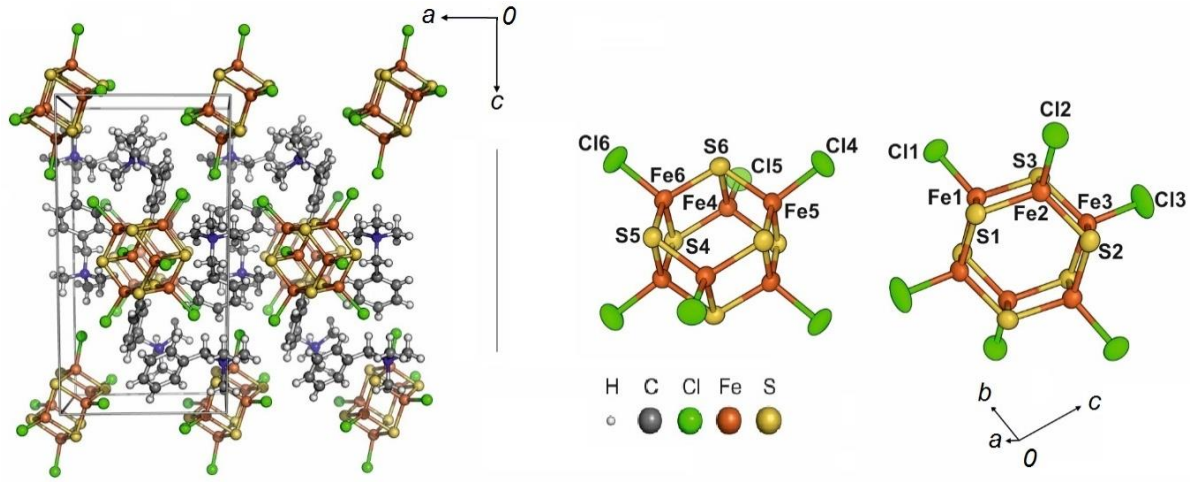

Fig. S2 Crystal structure of $(BTMA)_3[Fe_6S_6Cl_6]$ (**6**) (left; viewed along crystallographic *b* axis) and views on the prismane cluster trianions $[Fe_6S_6Cl_6]^{3-}$ (right).

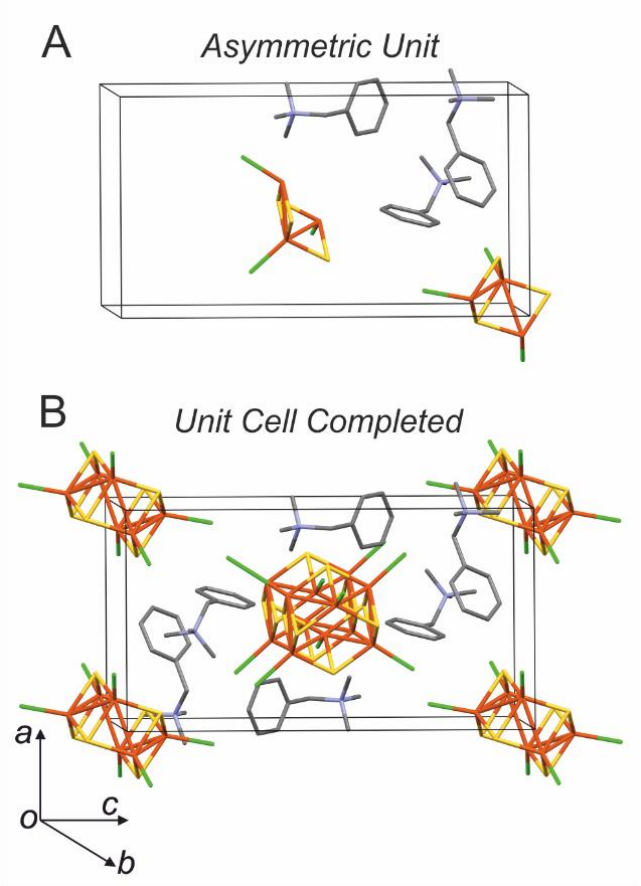

Fig. S3 Asymmetric unit for the crystal structure of $(BTMA)_3[Fe_6S_6Cl_6]$ (**6**) (**A**) and completed unit cell (**B**).

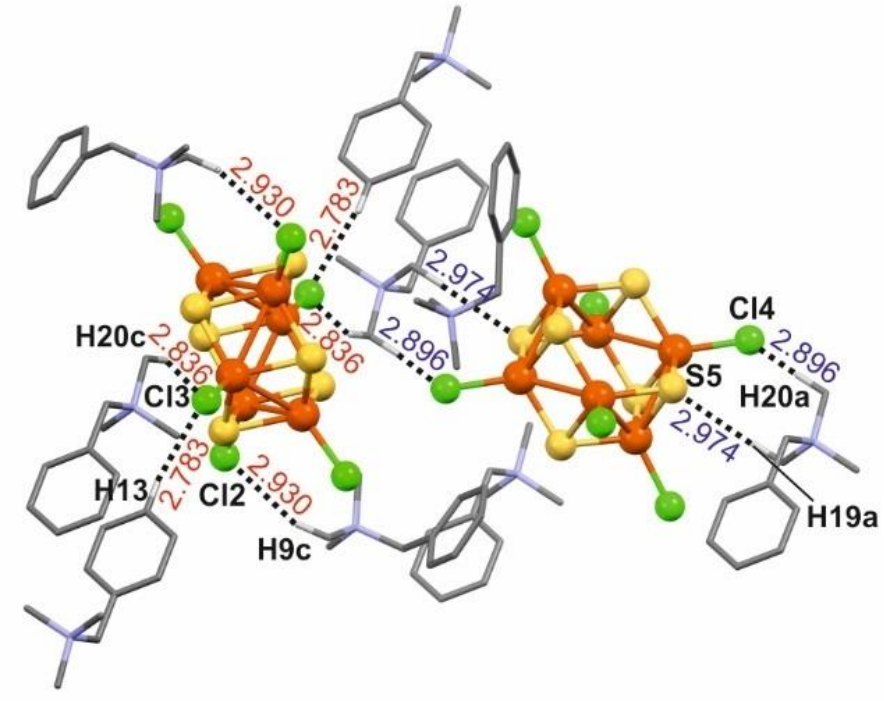

Fig. S4 Intermolecular interactions in $(BTMA)_3[Fe_6S_6Cl_6]$ (**6**). Only H atoms involved in the short contacts are shown; distances are in Å.

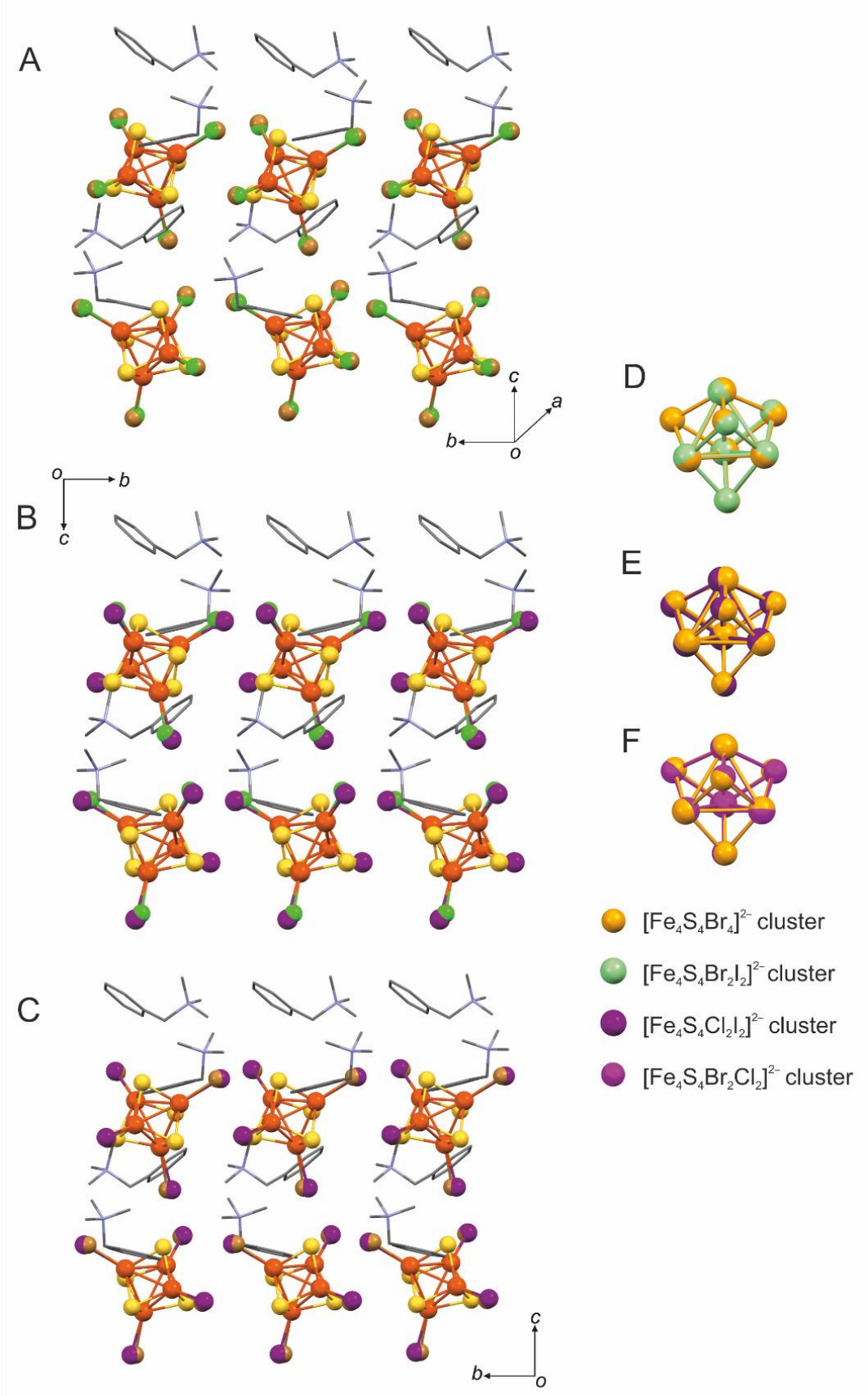

Fig. S5 Orientation of the mixed-halide compounds $(BTMA)_2[Fe_4S_4X_2Y_2]$ (**A**: Cl_2Br_2, **B:** Br_2I_2, **C:** Cl_2I_2), viewed along the crystallographic *a* axis and overlaid cores of the mixed-halide clusters (**D**, **E**, and **F**).

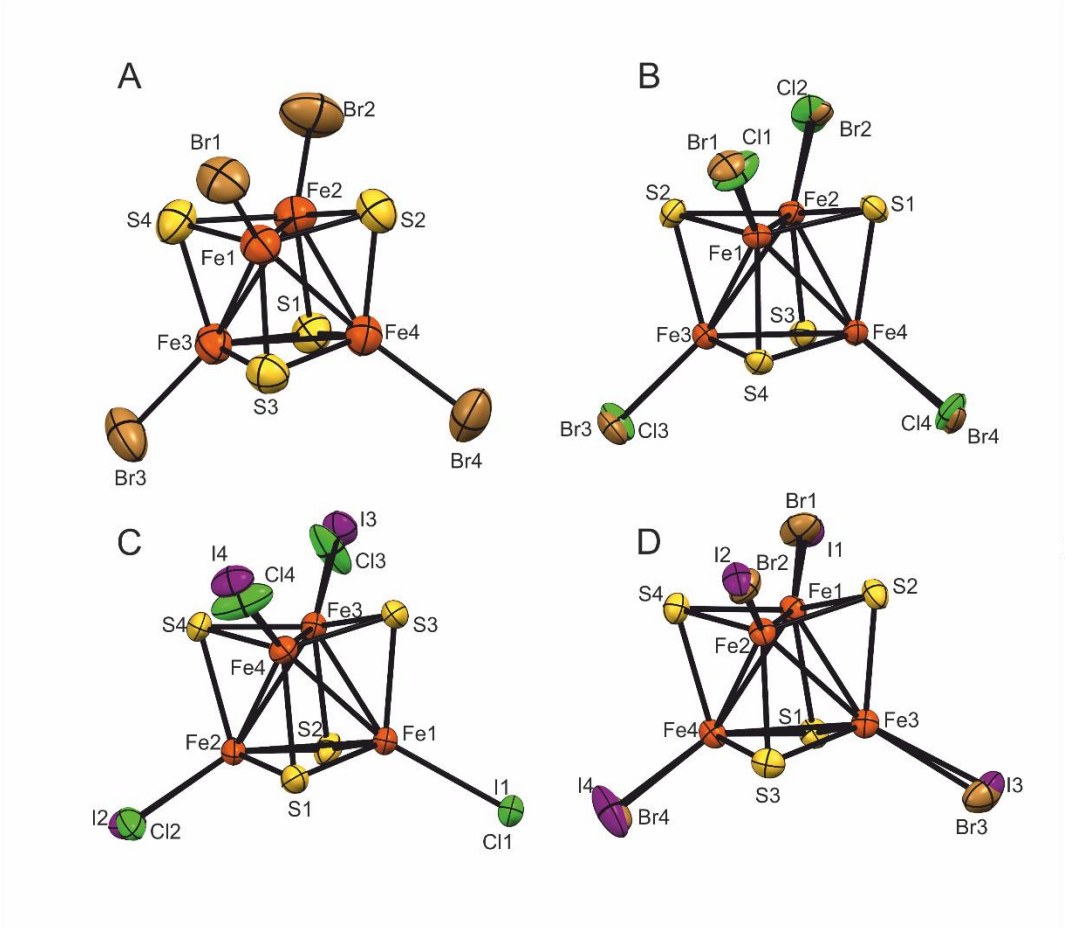

Fig. S6 Split occupancies and numbering for the $[Fe_4S_4Br_4]^{2-}$ (A) and the mixed-halide clusters $[Fe_4S_4X_2Y_2]^{2-}$ (B, C, and D) with selected Fe…Fe distances (from single crystal XRD of $(BTMA)_2[Fe_4S_4X_{4-x}Y_x]$ (X, Y = Cl, Br, I; x = 0 or 2) at 173 K.

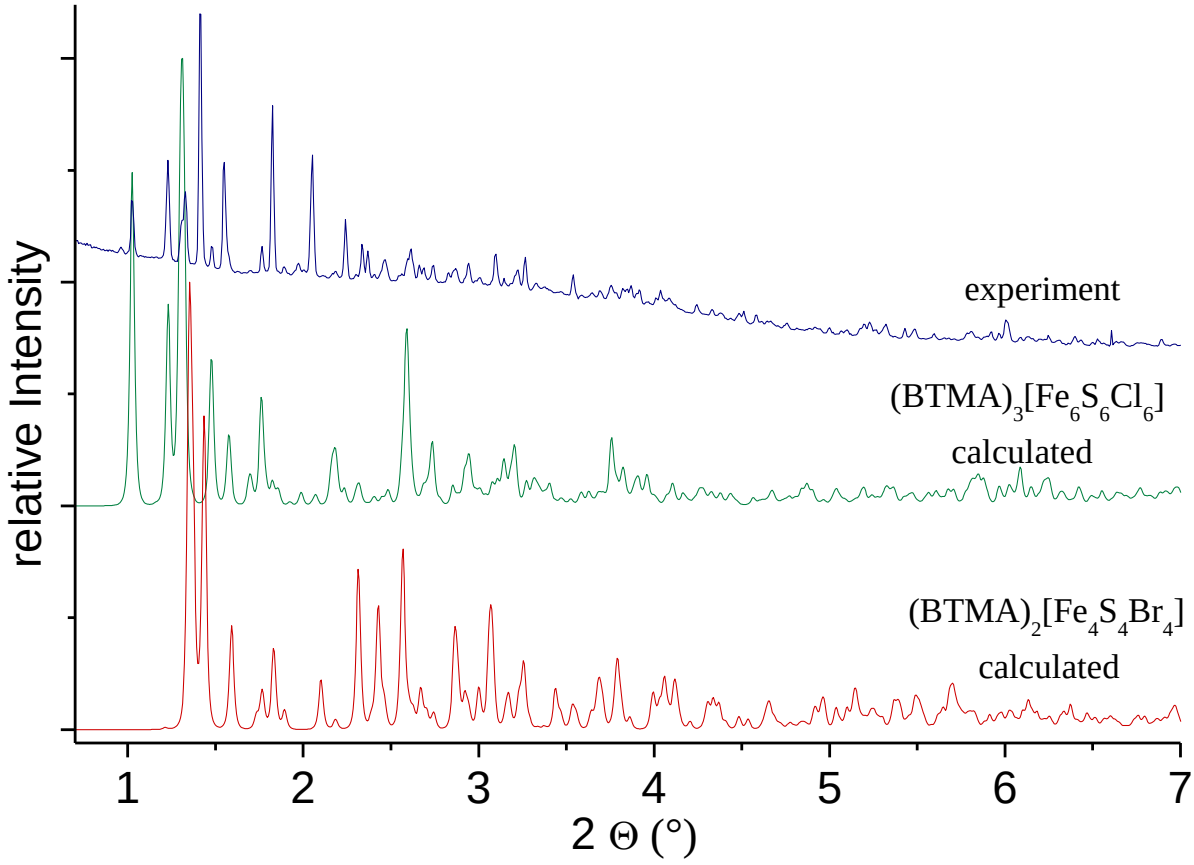

Fig. S7 Powder X-ray diffractogram of $(BTMA)_3[Fe_6S_6Cl_6]$ (**6**) recorded at 298 K (Beamline P02.1, DESY, Hamburg/Germany; λ = 0.207203 Å). For comparison, the simulated PXRD patterns of $(BTMA)_3[Fe_6S_6Cl_6]$ (**6**) and $(BTMA)_2[Fe_4S_4Br_4]$ (**1**) calculated from the known single crystal XRD data are shown.

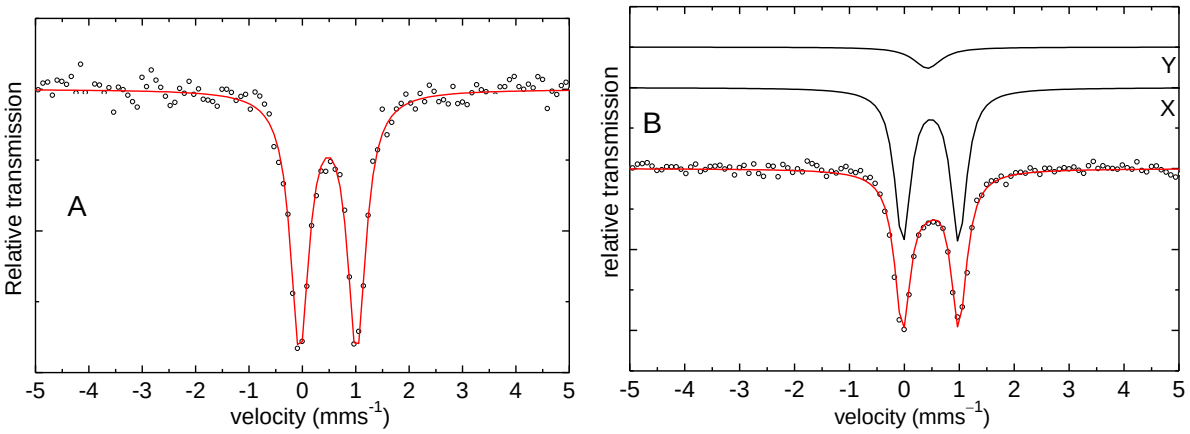

Fig. S8 ^{57}Fe Mössbauer spectra of $(BTMA)_2[Fe_4S_4Br_4]$ (**1**) (A) and $(BTMA)_2[Fe_4S_4I_4]$ (**5**) (B) at 77 K (dots: collected data, red line curve fits with parameters given in Table 3 in the manuscript or in the text). The minor species Y in the B plot with δ = 0.42 mm·s^{-1}, ΔE_Q = 0 mms^{-1} and Γ = 0.61 mm·s^{-1} accounts to 11% and has parameters typical of $(NEt_4)[FeI_4]$.[2]

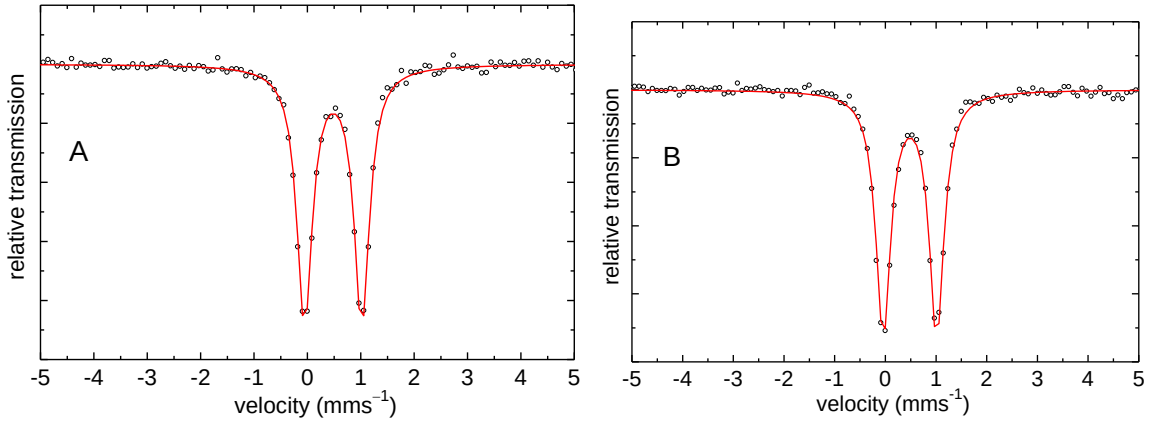

Fig. S9 ^{57}Fe Mössbauer spectra of (BTMA)$_2$[Fe$_4$S$_4$Br$_2$Cl$_2$] (**2**) (A) and (BTMA)$_2$[Fe$_4$S$_4$Br$_2$I$_2$] (**4**) (B) at 77 K (dots: collected data, red line curve fit with parameters given in Table 3).

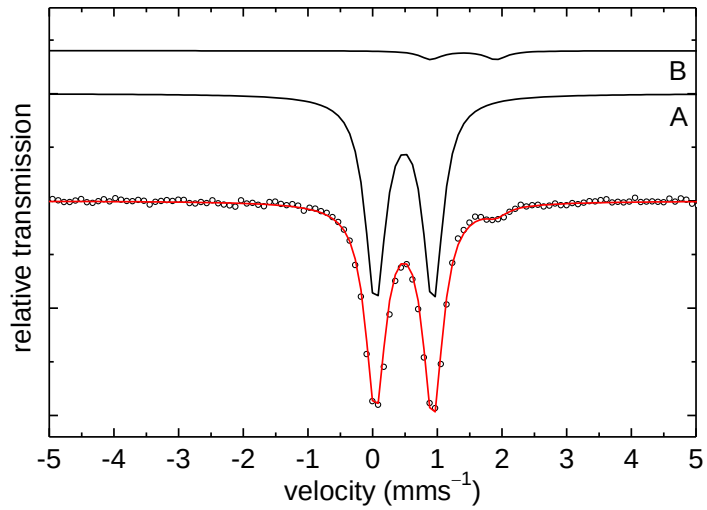

Fig. S10 ^{57}Fe Mössbauer spectrum of (BTMA)$_3$[Fe$_6$S$_6$Cl$_6$] (**6**) at 77 K (dots: collected data, red line curve fit with parameters given in Table 3). The minor species B with δ = 1.40 mm·s^{-1}, ΔE_Q = 1.01 mms^{-1}, and Γ = 0.40 mm·s^{-1} accounts to 4% and has parameters typical of FeCl$_2$.[3]

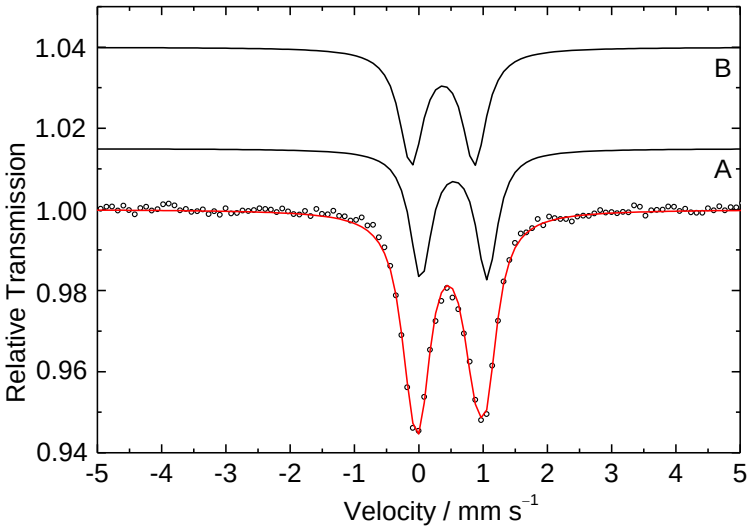

Fig. S11 ^{57}Fe Mössbauer spectrum of (BTMA)$_2$[Fe$_4$S$_4$Cl$_2$I$_2$] (**3**) at 77 K analysed with two "crossed" doublets and a relative area of 1:1 (dots: collected data, black line curve A: fit with δ_A = 0.54 mm s^{-1}, ΔE_{QA} = 1.03 mm s^{-1}, Γ_A = 0.40 mm s^{-1} and B: δ_B = 0.37 mm s^{-1}, ΔE_{QB} = 0.98 mm s^{-1}, Γ_B = 0.45 mm s^{-1}.

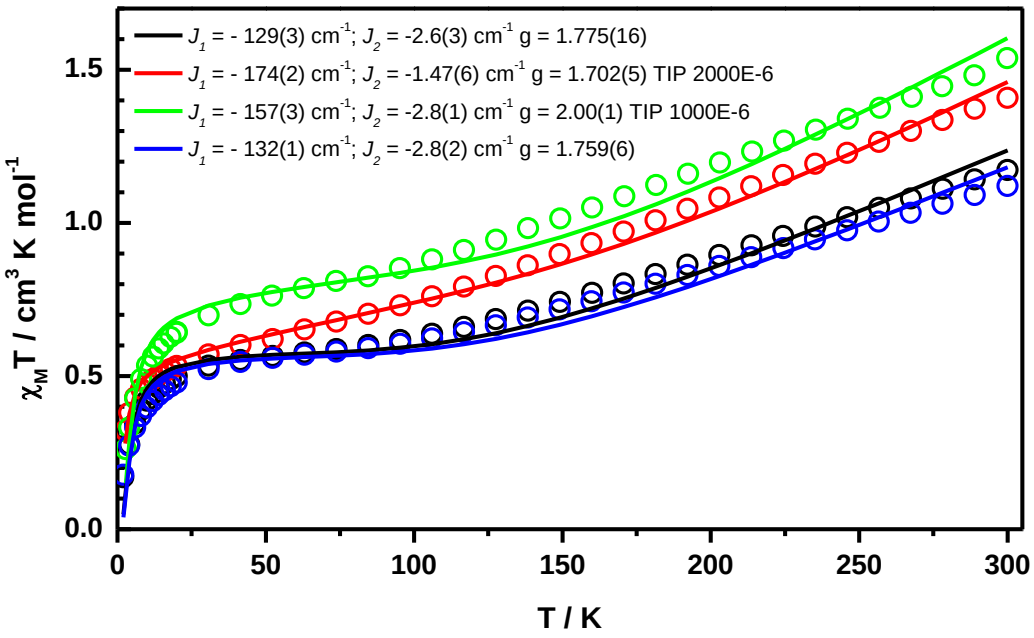

Fig. S12 Temperature dependence of molar magnetic susceptibility depicted as $\chi_M T$ vs. T for homoleptic cluster $(BTMA)_2[Fe_4S_4Br_4]$ (**1**) (black) and heteroleptic clusters $(BTMA)_2[Fe_4S_4Br_2Cl_2]$ (**2**) (green), $(BTMA)_2[Fe_4S_4Cl_2I_2]$ (**3**) (red), and $(BTMA)_2[Fe_4S_4Br_2I_2]$ (**4**) (blue). The solid lines correspond to the best fit obtained with the HDvV-Hamiltonian with the given parameter J_1, J_2, and g. Additional a TIP was included for $(BTMA)_2[Fe_4S_4Br_2Cl_2]$ (**2**) (green) and $(BTMA)_2[Fe_4S_4Cl_2I_2]$ (**3**) (red).

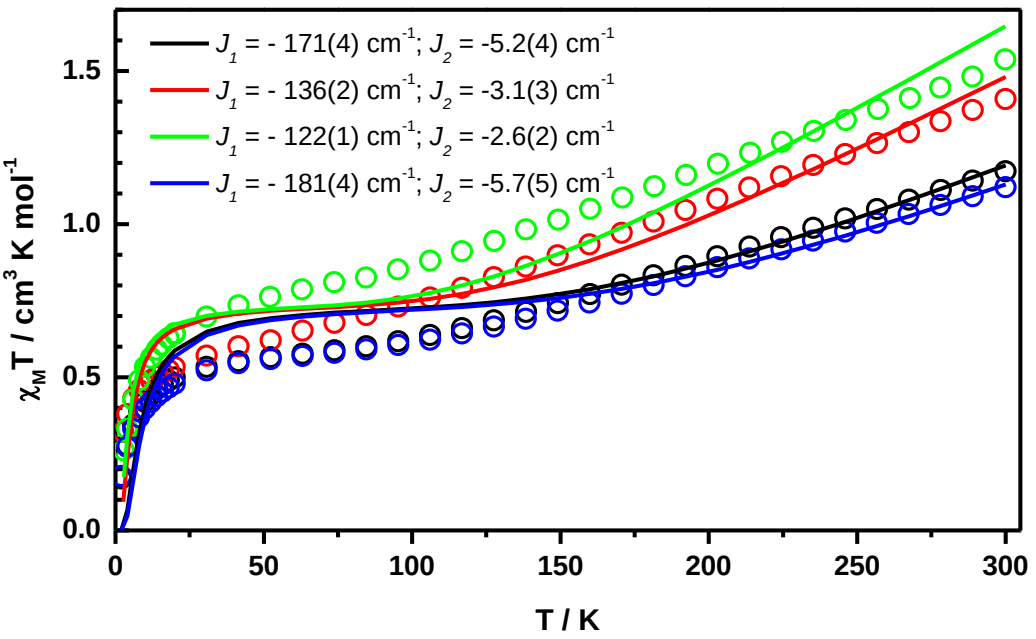

Fig. S13 Temperature dependence of molar magnetic susceptibility depicted as $\chi_M T$ vs. T for homoleptic cluster $(BTMA)_2[Fe_4S_4Br_4]$ (**1**) (black) and heteroleptic clusters $(BTMA)_2[Fe_4S_4Br_2Cl_2]$ (**2**) (green), $(BTMA)_2[Fe_4S_4Cl_2I_2]$ (**3**) (red), and $(BTMA)_2[Fe_4S_4Br_2I_2]$ (**4**) (blue). The solid lines correspond to the best fit obtained with the HDvV-Hamiltonian with the given parameter J_1, J_2, and fixed $g = 2.00$.

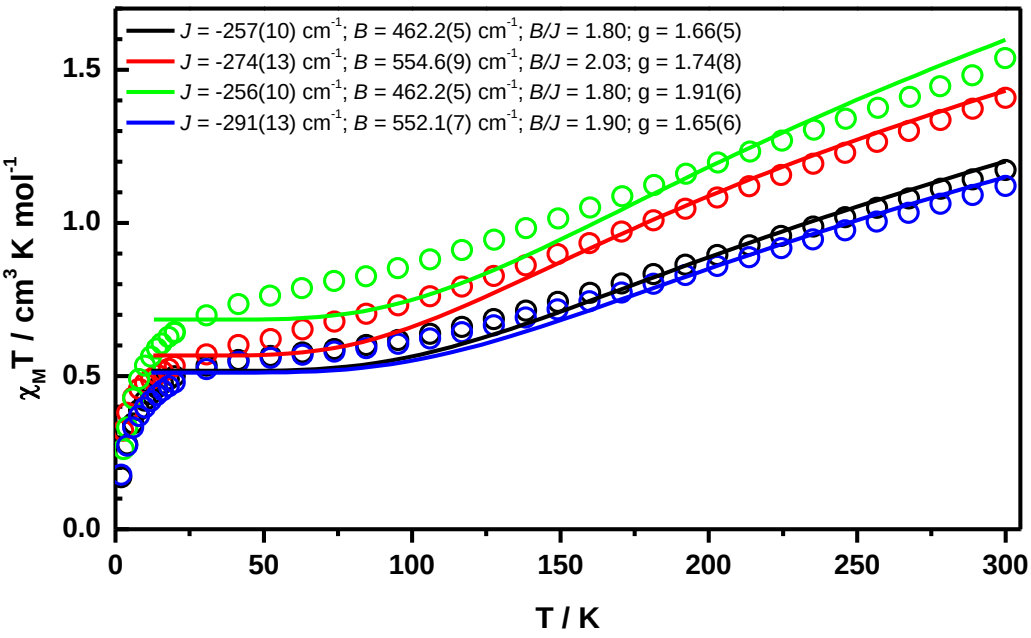

Fig. S14 Temperature dependence of molar magnetic susceptibility depicted as $\chi_M T$ vs. T for homoleptic cluster $(BTMA)_2[Fe_4S_4Br_4]$ (**1**) (black) and heteroleptic clusters $(BTMA)_2[Fe_4S_4Br_2Cl_2]$ (**2**) (green), $(BTMA)_2[Fe_4S_4Cl_2I_2]$ (**3**) (red), and $(BTMA)_2[Fe_4S_4Br_2I_2]$ (**4**) (blue). The solid lines correspond to the best fit obtained with the Bleany-Bowers equation derived from HDE with the given parameter J, B, and g.

Bleany-Bowers equation derived from the Heisenberg double-exchange (HDE)[10]:

$$E_{\pm} = -JS(S+1) \pm B(S+\tfrac{1}{2}) \quad (1)$$

$$\chi_M T = \frac{N_A g^2 \mu_B^2}{4k} \cdot \frac{e^{4y}(e^{2y}+1)+10e^{3x}(e^{7y}+e^{3y})+35e^{8x}(e^{8y}+e^{2y})+84e^{15x}(e^{9y}+e^{y})+165e^{24x}(e^{10y}+1)}{e^{4y}(e^{2y}+1)+2e^{3x}(e^{7y}+e^{3y})+3e^{8x}(e^{8y}+e^{2y})+4e^{15x}(e^{9y}+e^{y})+5e^{24x}(e^{10y}+1)} \quad (2)$$

$$x = -\frac{J}{kT}; y = -\frac{B}{kT}$$

C - Supporting Tables

Table S1. Selected crystallographic and refinement data for $(BTMA)_2[Fe_4S_4Br_4]$ (**1**).

	$(BTMA)_2[Fe_4S_4Br_4]$
T/K	293(2)
CCDC	2048374
empirical formula	$C_{20}H_{32}Br_4Fe_4N_2S_4$
formula weight/g·mol^{-1}	971.75
crystal system / space group	monoclinic / Cc
a/Å	12.9908(13)
b/Å	14.8857(13)
c/Å	17.3507(18)
β/°	95.318(8)
volume/Å^3 / Z	3340.8(6) / 4

ϱ_{calc}g/cm^3	1.932
μ/mm^{-1}	6.750
F(000)	1896.0
crystal size/mm^3	1.0 × 0.2 × 0.2
radiation	MoKα (λ = 0.71073 Å)
2Θ range for data collection/°	4.172 to 54.644
index ranges	–16 ≤ h ≤ 16, –19 ≤ k ≤ 19, –22 ≤ l ≤ 22
reflections collected	20221
independent reflections	7052 [R_{int} = 0.0426, R_{sigma} = 0.0329]
data/restraints/parameters	7052/2/308
goodness-of-fit on F^2	1.087
final R indexes [I>=2σ (I)]	R_1 = 0.0510, wR_2 = 0.1306
final R indexes [all data]	R_1 = 0.0682, wR_2 = 0.1494
largest diff. peak/hole / e Å^{-3}	0.59/–0.61
Flack parameter	–0.005(18)

Table S2 Essential metrics of $[Fe_4S_4Br_4]^{2-}$.[a]

distances	[Å]	distances	[Å]	distances	[Å]
Fe1–S2	2.292(4)	Fe3–S4	2.263(4)	Fe1···Fe2	2.776(2)
Fe1–S3	2.269(4)	Fe4–S1	2.303(4)	Fe1···Fe3	2.772(2)
Fe1–S4	2.305(4)	Fe4–S2	2.262(4)	Fe1···Fe4	2.769(2)
Fe2–S1	2.249(4)	Fe4–S3	2.297(3)	Fe2···Fe3	2.759(3)
Fe2–S2	2.299(4)	Fe1–Br1	2.354(2)	Fe2···Fe4	2.748(2)
Fe2–S4	2.300(4)	Fe2–Br2	2.332(2)	Fe3···Fe4	2.717(2)
Fe3–S1	2.292(3)	Fe3–Br3	2.332(2)		
Fe3–S3	2.300(4)	Fe4–Br4	2.340(2)		
angles	[°]	angles	[°]	angles	[°]
Br3–Fe3–Fe1	148.63(9)	Br2–Fe2–Fe3	147.03(10)	Br1–Fe1–Fe4	150.38(10)
Br3–Fe3–Fe2	145.71(10)	Br2–Fe2–Fe4	145.79(11)	Br4–Fe4–Fe1	151.03(10)
Br3–Fe3–Fe4	138.53(10)	Br1–Fe1–Fe2	140.06(10)	Br4–Fe4–Fe2	143.34(9)
Br2–Fe2–Fe1	141.45(10)	Br1–Fe1–Fe3	144.61(9)	Br4–Fe4–Fe3	138.03(10)
S1–Fe4–Br4	108.30(11)	S3–Fe3–Br3	113.41(12)	S4–Fe2–Br2	114.30(13)
S2–Fe4–Br4	120.03(12)	S4–Fe3–Br3	119.66(12)	S2–Fe1–Br1	115.70(12)
S3–Fe4–Br4	115.17(12)	S1–Fe2–Br2	116.39(12)	S3–Fe1–Br1	118.87(12)
S1–Fe3–Br3	110.25(11)	S2–Fe2–Br2	113.43(13)	S4–Fe1–Br1	110.62(12)
Fe2–S1–Fe3	74.83(11)	Fe1–S2–Fe4	75.11(12)	Fe3–S3–Fe4	72.46(11)
Fe2–S1–Fe4	74.24(11)	Fe2–S2–Fe4	74.08(12)	Fe1–S4–Fe2	73.93(11)
Fe3–S1–Fe4	72.50(11)	Fe1–S3–Fe3	74.69(12)	Fe1–S4–Fe3	74.72(12)
Fe1–S2–Fe2	74.19(12)	Fe1–S3–Fe4	74.87(11)	Fe2–S4–Fe3	74.42(11)

[a] From single crystal XRD of $(BTMA)_2[Fe_4S_4Br_4]$ (Table S1).

Table S3. Selected crystallographic and refinement data for $(BTMA)_2[Fe_4S_4X_2Y_2]$ with X,Y = Cl, Br, I.[a]

	$(BTMA)_2[Fe_4S_4Br_2Cl_2]$		**$(BTMA)_2[Fe_4S_4Cl_2I_2]$**	
T in K	293(2)	173(2)	293(2)	173(2)
CCDC	2048953	2048376	2048954	2048375
empirical formula	$C_{20}H_{32}Br_{2.09}Cl_{1.91}Fe_4N_2S_4$	$C_{20}H_{32}Br_2Cl_2Fe_4N_2S_4$	$C_{20}H_{32}Cl_{1.65}Fe_4I_{2.35}N_2S_4$	$C_{20}H_{32}Cl_{1.76}Fe_4I_{2.24}N_2S_4$
formula weight in g·mol^{-1}	886.95	882.83	1008.59	998.53
crystal system / space group	monoclinic / *Cc*	monoclinic / *Cc*	monoclinic / *Cc*	monoclinic / *Cc*
a/Å	12.8775(5)	12.79122(18)	13.1754(3)	13.0899(4)
b/Å	14.7140(6)	14.6187(2)	14.7340(4)	14.6471(4)
c/Å	17.3223(7)	17.1838(2)	17.5672(4)	17.4361(5)
β/°	95.142(3)	94.8717(13)	96.3025(19)	96.225(3)
volume in Å^3 / Z	3269.01(22) / 4	3201.62(8) / 4	3389.65(14) / 4	3323.28(18) / 4
ϱ_{calc}g in cm^3	1.802	1.832	1.976	1.996

μ in mm^{-1}	4.726	4.714	4.206	4.197
F(000)	1759.0	1752.0	1946.0	1930.0
crystal size in mm^3	0.5 × 0.4 × 0.3	0.098 × 0.049 × 0.012	0.8 × 0.4 × 0.3	0.14 × 0.06 × 0.04
2Θ range for data collection in °	4.212 to 53.658	7.642 to 59.02	7.358 to 58.982	7.906 to 58.966
index ranges	–16 ≤ h ≤ 16, –18 ≤ k ≤ 18, –21 ≤ l ≤ 21	–17 ≤ h ≤ 17, –20 ≤ k ≤ 20, –23 ≤ l ≤ 23	–16 ≤ h ≤ 17, –19 ≤ k ≤ 19, –23 ≤ l ≤ 24	–18 ≤ h ≤ 16, –19 ≤ k ≤ 19, –23 ≤ l ≤ 21
reflections collected	22278	24700	25715	23842
independent reflections	6579 [R_{int} = 0.0637, R_{sigma} = 0.0403]	7728 [R_{int} = 0.0354, R_{sigma} = 0.0405]	8159 [R_{int} = 0.0810, R_{sigma} = 0.0810]	7917 [R_{int} = 0.0428, R_{sigma} = 0.0491]
data/restraints/parameters	6579/2/311	7728/2/372	8159/2/344	7917/4/373
goodness-of-fit on F^2	1.074	1.044	1.036	1.003
final R indexes [I>=2σ (I)]	R_1 = 0.0446, wR_2 = 0.1171	R_1 = 0.0289, wR_2 = 0.0487	R_1 = 0.0493, wR_2 = 0.0982	R_1 = 0.0302, wR_2 = 0.0488
final R indexes [all data]	R_1 = 0.0493, wR_2 = 0.1212	R_1 = 0.0377, wR_2 = 0.0512	R_1 = 0.1003, wR_2 = 0.1275	R_1 = 0.0390, wR_2 = 0.0528
largest diff. peak/hole in e $Å^{-3}$	0.41/–0.41	0.35/–0.34	0.54/–0.72	0.44/–0.36
Flack parameter	–0.012(19)	–0.020(9)	–0.05(4)	–0.020(18)

[a] Radiation: MoKα (λ = 0.71073 Å).

Table S4. Selected crystallographic and refinement data for $(BTMA)_2[Fe_4S_4Br_2I_2]$

	$(BTMA)_2[Fe_4S_4Br_2I_2]$	
T in K	293(2)	173(2)
CCDC	2055695	2048378
empirical formula	$C_{20}H_{32}Br_{2.12}Fe_4I_{1.88}N_2S_4$	$C_{20}H_{32}Br_2Fe_4I_2N_2S_4$
formula weight in $g{\cdot}mol^{-1}$	1059.86	1065.73
crystal system / space group	monoclinic / *Cc*	monoclinic / *Cc*
a/Å	13.210(2)	13.0906(3)
b/Å	14.957(2)	14.8245(3)
c/Å	17.513(2)	17.3176(4)
β/°	96.12(3)	95.942(2)
volume in $Å^3$ / Z	3440.5(2) / 4	3342.63(12) / 4
ϱ_{calc}g in cm^3	2.046	2.118
μ in mm^{-1}	6.060	6.203
F(000)	2031.0	2040.0
crystal size in mm^3	0.5 × 0.4 × 0.3	0.093 × 0.037 × 0.02
radiation	MoKα (λ = 0.71073 Å)	MoKα (λ = 0.71073 Å)
2Θ range for data collection in °	4.126 to 54.608	7.254 to 59.164
index ranges	–17 ≤ h ≤ 16, –19 ≤ k ≤ 19, –22 ≤ l ≤ 22	–18 ≤ h ≤ 17, –20 ≤ k ≤ 20, –24 ≤ l ≤ 23
reflections collected	26772	72621
independent reflections	7401 [R_{int} = 0.0355, R_{sigma} = 0.0225]	8613 [R_{int} = 0.0451, R_{sigma} = 0.0290]
data/restraints/parameters	7401/2/312	8613/4/358
goodness-of-fit on F^2	1.062	1.046
final R indexes [I>=2σ (I)]	R_1 = 0.0365, wR_2 = 0.0892	R_1 = 0.0237, wR_2 = 0.0399
final R indexes [all data]	R_1 = 0.0439, wR_2 = 0.0960	R_1 = 0.0305, wR_2 = 0.0421
largest diff. peak/hole in e $Å^{-3}$	0.69/–0.61	0.37/–0.40
Flack parameter	0.017(12)	–0.021(9)

Table S5 Selected metrics of $(BTMA)_2[Fe_4S_4X_4]$ and $(BTMA)_2[Fe_4S_4X_2Y_2]$ with X,Y = Cl, Br, I, Part I.

	$[Fe_4S_4Br_4]^{2-}$	$[Fe_4S_4Br_2Cl_2]^{2-}$		$[Fe_4S_4Cl_2I_2]^{2-}$		$[Fe_4S_4Br_2I_2]^{2-}$		$[Fe_4S_4I_4]^{2-}$ [a]
δ in g/cm^3	1.932	1.802		1.976		2.046		2.192
distances	in Å	in Å		in Å		in Å		in Å
T in K	293	293	173	293	173	293	173	293
Fe(1)···Fe(2)	2.776(2)	2.775(2)	2.738(1)	2.767(2)	2.748(1)	2.766(2)	2.718(1)	2.759(2)

Fe(1)···Fe(3)	2.772(2)	2.773(2)	2.750(1)	2.760(2)	2.748(1)	2.765(2)	2.703(1)	2.756(2)
Fe(1)···Fe(4)	2.769(2)	2.765(2)	2.767(1)	2.758(3)	2.751(1)	2.758(2)	2.749(1)	2.754(2)
Fe(2)···Fe(3)	2.759(3)	2.762(2)	2.763(1)	2.750(2)	2.755(1)	2.757(2)	2.746(1)	2.750(2)
Fe(2)···Fe(4)	2.748(2)	2.748(2)	2.738(1)	2.734(3)	2.731(1)	2.735(2)	2.742(1)	2.726(2)
Fe(3)···Fe(4)	2.717(2)	2.725(2)	2.719(1)	2.725(3)	2.731(1)	2.716(2)	2.737(1)	2.696(2)
avd. value	2.757(22)	2.758(2)	2.746(1)	2.749(2)	2.744(1)	2.749(8)	2.733(1)	2.740(2)
Fe1–X/Y	2.354(2)	2.335(2)	2.210(1) 2.323(5)	2.548(2)	2.551(1)	2.524(1)	2.367(1) 2.514(1)	2.557(2)
Fe2–X/Y	2.332(2)	2.295(2)	2.342(3) 2.340(2)	2.500(5) 2.495(4)	2.248(1) 2.360(2)	2.477(1)	2.409(1) 2.545(4)	2.522(2)
Fe3–X/Y	2.332(2)	2.284(2)	2.223(1) 2.330(1)	2.230(2) 2.340(3)	2.2400(2) 2.5126(2)	2.380(2)	2.452(1) 2.479(4)	2.520(3)
Fe4–X/Y	2.340(2)	2.256(2)	2.200(1) 2.316(1)	2.560(3) 2.399(1)	2.237(15) 2.483(4)	2.438(2)	2.368(4) 2.411(1)	2.495(3)
X/Y···X/Y[b] distances between clusters	Br3···Br4 3.814(2) Br2···Br4 4.871(3) Br1···Br2 5.238(3) Br1···Br4 5.328(3)	Br/Cl3···Br/Cl4 3.75(2) Br/Cl2···Br/Cl4 5.299(2) Br/Cl1···Br/Cl2 5.161(2) Br/Cl1···Br4Cl4 5.439(3)	Br/Cl3···Br/Cl4 3.75(2) Br/Cl2···Br/Cl4 5.39(3) Br/Cl1···Br/Cl2 5.18(3) Br/Cl1···Br/Cl4 5.25(4)	I/Cl3···I/Cl4 3.80(4) I/Cl2···I/Cl4 4.77(4) Br/Cl1···I/Cl2 4.87(3) I/Cl1···I/Cl4 5.31(3)	I/Cl3···I/Cl4 3.74(2) I/Cl1···I/Cl3 4.87(2) Br/Cl1···I/Cl2 4.952(6) I/Cl1···I/Cl4 5.30(3)	I/Br3···I/Br4 3.849(25) I/Br2···I/Br4 5.340 (1) Br/Br1···I/Br2 5.086(1) I/Br1···I4Br4 6.987(2)	I/Br3···I/Br4 3.79(3) I/Br1···I/Br3 4.59 (5) Br/Br1···I/Br2 5.137(14) I/Br1···I/Br4 5.27(3)	I3···I4 3.918(2) I2···I3 4.510 I1···I4 5.121 I1···I3 5.413(2)

[a] From Ref. 6. [b] Shorter distances; for mixed clusters, distances correspond to the average values.

Table S6 Selected metrics of $(BTMA)_2[Fe_4S_4X_4]$ and $(BTMA)_2[Fe_4S_4X_2Y_2]$ with X,Y = Cl, Br, I, Part II.

column	1	2	3	4	5	6	7	8	9	10
	Br_4	Δ to av.	**Br_2Cl_2**	Δ to av.			**Cl_2I_2**	Δ to av.		
δ in g/cm^3	1.932		1.802				1.976			
T in K	293		293		173		293		173	
Fe(1)···Fe(2)	2.776(2)	+0.019	2.775(2)	+0.017	2.767(1)	+0.021	2.767(2)	+0.018	2.755(1)	+0.011
Fe(1)···Fe(3)	2.772(2)	+0.015	2.773(2)	+0.015	2.763(1)	+0.017	2.760(2)	+0.011	2.751(1)	+0.007
Fe(1)···Fe(4)	2.769(2)	+0.012	2.765(2)	+0.007	2.750(1)	+0.004	2.758(3)	+0.009	2.748(1)	+0.005
Fe(2)···Fe(3)	2.759(3)	+0.002	2.762(2)	+0.004	2.738(1)	–0.008	2.750(2)	+0.001	2.748(1)	+0.004
Fe(2)···Fe(4)	2.748(2)	–0.009	2.748(2)	–0.010	2.738(1)	–0.008	2.734(3)	–0.006	2.731(1)	–0.013
Fe(3)···Fe(4)	2.717(2)	–0.040	2.725(2)	–0.033	2.719(1)	–0.027	2.725(3)	–0.024	2.731(1)	–0.013
avd. value	2.757(2)		2.758(2)		2.746(1)		2.749(2)		2.744(1)	
largest Δ [a]	0.059		0.050		0.048		0.042		0.024	

column	11	12	13	14	15	16
	Br_2I_2	Δ to av.			**I_4** [a]	Δ to av.
δ in g/cm^3	2.046				2.192	
T in K	293		173		293	
Fe(1)···Fe(2)	2.766(2)	+0.017	2.749(1)	+0.016	2.759(3)	+0.019
Fe(1)···Fe(3)	2.765(2)	+0.016	2.746(1)	+0.013	2.756(2)	+0.016
Fe(1)···Fe(4)	2.757(2)	+0.008	2.742(1)	+0.009	2.754(3)	+0.014
Fe(2)···Fe(3)	2.758(2)	+0.009	2.737(1)	+0.004	2.750(3)	+0.010
Fe(2)···Fe(4)	2.735(2)	–0.014	2.718(1)	–0.015	2.726(3)	–0.014
Fe(3)···Fe(4)	2.716(2)	–0.033	2.703(1)	–0.030	2.696(3)	–0.440
avd. value	2.749(8)		2.733(1)		2.740(2)	
largest Δ [a]	0.050		0.043		0.063	

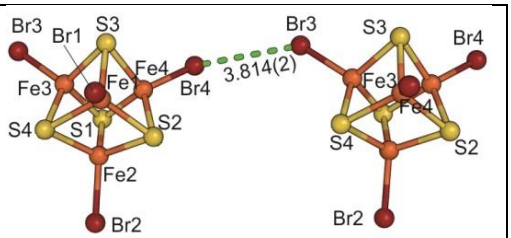

numbering scheme

[a] Difference between smallest and largest value. [b] From Ref. 4.

Table S7 Metrical data showing the Fe_4 tetrahedron distortion and compression in $(Q)_2[Fe_4S_4X_4]$ and $(Q)_2[Fe_4S_4X_2Y_2]$ structures with X, Y = Cl, Br, I and Q = Ph_4P^+, Et_4N^+, and nPr_4N^+.

	Ph_4P^+					Et_4N^+	nPr_4N^+
cluster	$[Fe_4S_4Cl_4]^{2-}$	$[Fe_4S_4Br_2Cl_2]^{2-}$	$[Fe_4S_4Br_4]^{2-}$	$[Fe_4S_4I_4]^{2-}$	$[Fe_4S_4(SH)_4]^{2-}$	$[Fe_4S_4Cl_4]^{2-}$	$[Fe_4S_4Cl_4]^{2-}$
refs	[5]	[5]	[5]	[6]	[7]	[8]	[9]
space group	*C*2/c	*C*2/c	*C*2/c	$I4_1/a$	*C*2/c	$P2_1/c$	$P2_1/n$
density in g/cm³	1.55	1.65	1.76	1.90	1.50	1.63	1.45
T in K	294	294	294	283–303	294	283–303	213
distances in Å							
Fe(1)···Fe(2)	2.778(1)	2.777(2)	2.767(2)	2.743(2)	2.770(3)	2.777(1)	2.789(1)
Fe(1)···Fe(1b)	2.775(2)	2.765(4)	2.747(3)	2.755(2)	2.762(4)	2.746(1)	2.769(1)
Fe(1)···Fe(2b)	2.773(1)	2.769(3)	2.760(2)	2.755(2)	2.769(3)	2.776(1)	2.770(1)
Fe(1b)···Fe(2b)	2.773(1)	2.769(3)	2.760(2)	2.755(2)	2.769(3)	2.765(1)	2.768(1)
Fe(2)···Fe(2b)	2.751(2)	2.760(3)	2.767(2)	2.755(2)	2.738(3)	2.764(1)	2.771(1)
Fe(2)···Fe(1b)	2.778(1)	2.777(2)	2.767(2)	2.743(2)	2.770(3)	2.765(1)	2.753(1)
averaged value	2.771(10)	2.770(7)	2.761(8)	2.751(6)	2.763(13)	2.766(11)	2.770(12)
largest Δ in Å[a]	0.027	0.017	0.020	0.012	0.032	0.031	0.036
Fe–X	2.204(3) 2.211(3)	2.321(3) (Br/Cl) 2.291(3) (Br/Cl)	2.338(2) 2.345(2)	2.541(1)	2.269(5) 2.256(4)	2.216	2.210(1) 2.212(1) 2.197(1)
X···X distances between clusters	No data available	No data available	4.040(1) 6.846(1) 6.874(1)	4.336(1) 6.441(1) 9.163(1)	4.240(1)	3.964(1) 4.599(1) 4.751(1) 5.536(1)	4.391(1) 4.711(1) 7.113(1)

[a] Difference between smallest and largest value.

Table S8 Selected crystallographic and refinement data for $(BTMA)_3[Fe_6S_6Cl_6]$ (**6**)

formula	$C_{30}H_{48}Cl_6Fe_6N_3S_6$	radiation	MoKα (λ = 0.71073 Å)
formula weight in g·mol⁻¹	1190.87	*T* in K	293(2)
size in mm	1.0 × 0.5 × 0.3	F(000)	1206.0
crystal system	triclinic	ϱ_{calc}g/cm³	1.626
space group	$P\bar{1}$	2Θ range data collection/°	3.418 to 53.628
a/Å	10.2381(5)	index ranges	–11 ≤ h ≤ 12, –15 ≤ k ≤ 15, –25 ≤ l ≤ 25
b/Å	12.3598(6)	reflections collected	33479
c/Å	19.934(1)	independent reflections	10306 [R_{int} = 0.1106, R_{sigma} = 0.0729]
α/°	104.898(4)	data/restraints/parameters	10306/0/469
β/°	89.793(4)	goodness-of-fit on F^2	0.998
γ/°	93.675(4)	final R indexes [I>=2σ (I)]	R_1 = 0.0387, wR_2 = 0.0938
Volume in Å³ / Z	2432.4(2) / 2	Final R indexes [all data]	R_1 = 0.0589, wR_2 = 0.1066
μ in mm⁻¹	2.354	Larg. diff. peak/hole in e Å⁻³	0.53/–0.61
CCDC	2048377		

Table S9 Essential metrics in $[Fe_6S_6Cl_6]^{3-}$.[a]

distances	in Å	distances	in Å	distances	in Å
Fe1–Cl1	2.2036(10)	Fe5–Cl5	2.1949(11)	Fe2···Fe3	2.7536(6)
Fe2–Cl2	2.2178(10)	Fe6–Cl6	2.2128(10)	Fe4···Fe5	2.7603(6)

Fe3–Cl3	2.2130(11)	Fe1···Fe2	2.7628(7)	Fe4···Fe6	2.7752(6)
Fe4–Cl4	2.2146(10)	Fe1···Fe3	2.7614(7)	Fe5···Fe6	2.7620(7)
Fe1–S1	2.2930(9)	Fe3–S1	2.2759(10)	Fe5–S4	2.2754(9)
Fe1–S2	2.2695(9)	Fe3–S2	2.2912(9)	Fe5–S5	2.2810(9)
Fe1–S3	2.2649(10)	Fe3–S3	2.2655(9)	Fe5–S6	2.2740(9)
Fe2–S1	2.2792(10)	Fe4–S4	2.2682(9)	Fe6–S4	2.2964(9)
Fe2–S2	2.2703(9)	Fe4–S5	2.2659(9)	Fe6–S5	2.2755(10)
Fe2–S3	2.2893(9)	Fe4–S6	2.2854(9)	Fe6–S6	2.2736(10)
angles	in °	angles	in °	angles	in °
Cl1–Fe1–S1	113.07(4)	S2–Fe1–S1	105.62(4)	Fe2–S1–Fe1	74.35(3)
Cl1–Fe1–S2	111.94(4)	S3–Fe1–S1	105.63(4)	Fe3–S1–Fe1	74.37(3)
Cl1–Fe1–S3	109.90(5)	S3–Fe1–S2	110.44(3)	Fe3–S1–Fe2	113.02(3)
Cl2–Fe2–S1	111.76(4)	S1–Fe2–S3	105.28(4)	Fe1–S2–Fe2	114.70(4)
Cl2–Fe2–S2	109.29(4)	S2–Fe2–S1	111.54(4)	Fe1–S2–Fe3	74.52(3)
Cl2–Fe2–S3	113.19(4)	S2–Fe2–S3	105.60(3)	Fe2–S2–Fe3	74.26(3)
Cl3–Fe3–S1	111.84(4)	S1–Fe3–S2	105.47(4)	Fe1–S3–Fe2	74.70(3)
Cl3–Fe3–S2	113.63(4)	S3–Fe3–S1	111.83(4)	Fe1–S3–Fe3	114.64(4)
Cl3–Fe3–S3	108.26(5)	S3–Fe3–S2	105.69(3)	Fe3–S3–Fe2	74.39(3)
Cl4–Fe4–S4	109.02(4)	S4–Fe4–S5	112.72(4)	Fe4–S4–Fe5	114.13(4)
Cl4–Fe4–S5	111.60(4)	S4–Fe4–S6	105.31(3)	Fe4–S4–Fe6	74.88(3)
Cl4–Fe4–S6	112.62(4)	S5–Fe4–S6	105.42(3)	Fe6–S4–Fe5	74.34(3)
Cl5–Fe5–S4	109.83(5)	S5–Fe5–S4	105.75(4)	Fe4–S5–Fe5	74.76(3)
Cl5–Fe5–S5	115.96(5)	S6–Fe5–S4	110.81(3)	Fe4–S5–Fe6	113.36(4)
Cl5–Fe5–S6	109.08(5)	S6–Fe5–S5	105.29(3)	Fe5–S5–Fe6	74.63(3)
Cl6–Fe6–S4	114.26(4)	S4–Fe6–S5	105.24(3)	Fe5–S6–Fe4	74.52(3)
Cl6–Fe6–S5	111.42(4)	S6–Fe6–S4	104.78(3)	Fe6–S6–Fe4	75.00(3)
Cl6–Fe6–S6	109.05(4)	S6–Fe6–S5	111.92(4)	Fe6–S6–Fe5	114.96(4)

[a] From single crystal XRD of $(BTMA)_3[Fe_6S_6Cl_6]$. Colour code: Fe–S between six-membered chairs; S–Fe–S inside chair; Fe–S–Fe inside chair.

Table S10 Freely refined halide ratios in $(BTMA)_2[Fe_4S_4X_2Y_2]$ structures.[a]

2		**3**		**4**	
Br	Cl	Cl	I	Br	I
2.00	2.00	1.76	2.24	2.00	2.00

[a] From a preliminary refinement with X and Y occupancies freely refined from single crystal XRD at 173 K (full final data from refinement using SUMP in Tables S3 and S4).

References

1 A. O. Schüren, V. K. Gramm, M. Dürr and A. Foi, I. Ivanović-Burmazović, F. Doctorovich, U. Ruschewitz and A. Klein, Halide coordinated homoleptic $[Fe_4S_4X_4]^{2-}$ and heteroleptic $[Fe_4S_4X_2Y_2]^{2-}$ clusters (X, Y = Cl, Br, I)—alternative preparations, structural analogies and spectroscopic properties in solution and solid state, *Dalton Trans.* 2016, **45**, 361–375.

2 D. J. Evans, G. García, M. D. Santana and M. C. Torralba, About the synthesis of the prismane $[NEt_4]_2[Fe_6S_6I_6]$, *Inorg. Chim. Acta* 1999, **284**, 296–299.

3 K. Ôno, A. Ito and T. Fujita, The Mössbauer Study of the Ferrous Ion in $FeCl_2$; *J. Phys. Soc. Jpn*. 1964, **19**, 2119–2126.

4 G. B. Wong, M. A. Bobrik and R. H. Holm, Inorganic Derivatives of Iron Sulfide Thiolate Dimers and Tetramers: Synthesis and Properties of the Halide Series $[Fe_2S_2X_4]^{2-}$ and $[Fe_4S_4X_4]^{2-}$ (X = Cl, Br, I), *Inorg. Chem.* 1978, **17**, 578–584.

5 A. Müller, N. H. Schladerbeck, E. Krickemeyer, H. Bögge, K. Schmitz, E. Bill and A. X. Trautwein, Darstellung von Metall-Schwefel-Clustern durch einfache Reaktion von Metallsalzen mit H_2S: $R_2(NH_4)[Cu_3S_{12}]$, $R_2[Cu_4S_{12}]\cdot CH_3CN$, $R_2[Cu_4S_{12.8}]$, $R_2[Fe_2S_2(S_5)_2]$, $R_2[Fe_4S_4Br_4]$, $R_2[Fe_4S_4Br_2Cl_2]$, $R_2[Fe_4S_4Cl_4]$, $R_2[Fe_2S_2Cl_4]$ (R = PPh_4) und $[Fe(DMF)_6][Fe_2S_2Cl_4]$, *Z. Anorg. Allg. Chem.* 1989, **570**, 7–36.

6 S. Pohl and W. Saak, Structural Distortion of $Fe_4S_4I_4^{2-}$ Clusters through Iodine-Iodine Contacts: Crystal Structures of $(Ph_4P)_2Fe_4S_4I_4$ and $(Me_3NCH_2Ph)_2Fe_4S_4I_4$, *Z. Naturforsch. b* 1988, **43b**, 457–462.

7 A. Müller, N. H. Schladerbeck and H. Bögge, $[Fe_4S_4(SH)_4]^{2-}$, the simplest synthetic analogue for a ferredoxin *Chem. Comunm.* **1987**, 35–36.

8 M. A. Bobrik, K. O. Hodgson and R. H. Holm, Inorganic Derivatives of Iron-Sulfide-Thiolate Dimers and Tetramers. Structures of Tetrachloro-*p*-disulfido-diferrate(III) and Tetrakis(chloro-μ_3-sulfido-iron) Dianions, *Inorg. Chem.* 1977, **16**, 1851–1858.

9 B. M. Segal, H. R. Hoveyda and R. H. Holm, Terminal Ligand Assignments Based on Trends in Metal-Ligand Bond Lengths of Cubane-Type$[Fe_4S_4]^{2+,+}$ Clusters. *Inorg. Chem.* 1998, **37**, 3440–3443.

10 J. T. Henthorn, G. E. Cutsail, T. Weyhermüller and S. DeBeer, Stabilization of intermediate spin states in mixed-valent diiron dichalcogenide complexes, *Nat. Chem.* 2022, **14**, 328–333.